International Journal of Applied Power Engineering (IJAPE)
Vol. 15, No. 3, September 2026, pp. 1200~1211
ISSN: 2252-8792, DOI: 10.11591/ijape.v15.i3.pp1200-1211

Multi-objective optimization and multi-criteria decision analysis of passive power filters for power quality improvement in arc furnace applications

Alvaro Yassif Marca Yucra, Gastón Orlando Suvire, John Armando Morales
Instituto de Energía Eléctrica, Universidad Nacional de San Juan (UNSJ)–CONICET, San Juan, Argentina

Article Info

Article history:

Received Sep 30, 2025
Revised Apr 1, 2026
Accepted Jun 10, 2026

Keywords:

Electric arc furnace
Harmonic distortion
Multi-objective optimization
Passive power filter
Steelmaking

ABSTRACT

This article presents a multi-objective optimization methodology for the optimal tuning of passive power filters in steelmaking facilities that operate with electric arc furnaces (EAFs). These industrial loads are well-known for introducing severe harmonic distortion, voltage unbalance, and flicker into the electrical network, significantly degrading power quality and equipment performance. To address these challenges, a multi-objective optimization problem is solved using the non-dominated sorting genetic algorithm II (NSGA-II), which simultaneously minimizes three key power quality indices: total harmonic distortion (THD), total demand distortion (TDD), and voltage unbalance factor (VUF). In addition, a multi-criteria decision analysis (MCDA) technique is applied to rank and select the most balanced and robust solution in different EAF operating scenarios. Unlike conventional filter design methods that prioritize a single performance criterion or rely on static harmonic assumptions, the proposed approach accounts for the nonlinear and time-varying behavior of EAFs, ensuring robust performance under diverse operating conditions. A comprehensive case study based on a Bolivian steel plant illustrates the effectiveness of the optimization strategy. Results indicate reductions of 47.6% in THD, 33.5% in TDD, and 63.6% in VUF, clearly outperforming conventional design approaches and significantly improving overall power quality. This work highlights the potential of evolutionary multi-objective algorithms for enhancing passive filter performance in complex industrial environments with highly distorted and unbalanced power conditions.

Corresponding Author:

Alvaro Yassif Marca Yucra
Instituto de Energía Eléctrica, Universidad Nacional de San Juan (UNSJ)–CONICET
Av. Libertador Gral. San Martín 1109, J5400 San Juan, Argentina
Email: alvaromarca25@gmail.com

1. INTRODUCTION

The steel industry faces the urgent challenge of reducing CO_2 emissions from smelting processes, in response to increasingly stringent environmental regulations [1]. In this context, electric arc furnaces (EAFs) have consolidated as a more sustainable alternative and are projected to become the dominant technology for steel production in the coming decades [2], [3]. However, their operation introduces significant disturbances into the electrical grid, such as harmonic distortion, voltage unbalance, and rapid voltage fluctuations (flicker). These conditions may increase energy losses within the plant's internal network, impair the performance of electrical equipment, and hinder compliance with power quality standards [4].

Currently, passive power filters (PPFs) are a widely used and cost-effective solution for mitigating harmonics in industrial networks. Their primary function is to reduce harmonic distortion and inject reactive power, which represents a fundamental step toward addressing power quality challenges in EAF-based systems. In addition, the reactive power injection inherently provided by PPFs helps improve the overall voltage profile, which in turn contributes to lowering voltage unbalance levels at the PCC.

Nevertheless, their performance is limited when facing the highly variable and nonlinear nature of loads such as EAFs, whose harmonic and interharmonic spectra dynamically fluctuate throughout the melting process [5], [6]. To overcome these limitations, several optimal filter design methodologies have been proposed, including classical nonlinear optimization approaches [7], [8], metaheuristic techniques such as particle swarm optimization (PSO) [9]-[11], and more recent methods such as simultaneous perturbation stochastic approximation (SPSA) and dynamic particle swarm optimization (DPSO) [12], [13]. Most of these studies, however, adopt a single-objective perspective, focusing exclusively on reducing harmonic indices without jointly addressing other equally critical indicators in EAF operation, such as voltage unbalance. Simultaneous mitigation of these indices is therefore crucial in industrial networks with EAFs, which are among the most disturbing loads in terms of power quality [14].

In this context, the present study proposes a methodology for the optimal tuning of a PPF in a steel plant operating with an EAF. The approach combines the non-dominated sorting genetic algorithm II with multi-criteria decision analysis. NSGA-II is adopted because of its proven efficiency in solving nonlinear multi-objective problems, its ability to approximate the Pareto front with good convergence and diversity, and its extensive use in power systems optimization. This makes it particularly suitable for addressing the conflicting objectives inherent to power quality improvement in EAF-based networks. The optimization problem is formulated as a nonlinear multi-objective problem, simultaneously minimizing three power quality indices: total harmonic distortion (THD), total demand distortion (TDD), and the voltage unbalance factor (VUF). The goal is to identify filter configurations that achieve an appropriate trade-off among these indicators, while ensuring robust performance under diverse operating conditions of the EAF melting process.

The main contribution of this work lies in the simultaneous minimization of THD, TDD, and VUF using NSGA-II combined with multi-criteria decision analysis (MCDA), which, to the best of our knowledge, has not been previously reported for EAF-based steelmaking facilities. This paper is structured as follows: Section 2 analyzes the operation of EAFs and their impact on power quality. Section 3 presents the proposed methodology, including the hyperbolic model of the furnace, the implementation of NSGA-II, and the adopted MCDA framework. Section 4 discusses the obtained results and compares the performance of the optimized design against conventional approaches. Finally, Section 5 summarizes the main conclusions of this work.

2. TECHNICAL BACKGROUND

2.1. Melting process in electric steelmaking furnaces

EAFs are fundamental equipment in modern steel plants, used to melt scrap steel through electric arcs exceeding 10 kA and temperatures above 3,000 °C. This process consumes large amounts of electrical energy and introduces significant disturbances into the power supply system [15]. The melting process comprises several stages, each with specific operating characteristics that affect power quality in different ways and with varying degrees of severity [16]. These stages can be divided into four main phases (Figure 1), each associated with distinct energy consumption patterns, arc dynamics, and impacts on the grid.

Figure 1. Main operating stages of the EAF steelmaking process

In the boring stage, the electrodes descend to establish the first arcs, piercing the upper scrap layer and creating a pit that enables heat penetration into the charge. This stage is highly unstable and generates severe fluctuations. During the melting stage, once the pit is formed, the electrodes are surrounded by scrap, allowing an increase in arc length and furnace power to accelerate melting—conditions that intensify harmonic distortion and reactive power demand. The plating stage begins when the molten bath is formed and the remaining solid material is melted. As the electrodes approach the molten bath, the arc stabilizes, reducing fluctuations but still contributing to distortion. Finally, in the refining stage, the charge is fully molten, and chemical and thermal adjustments are carried out, with a progressive reduction in arc length and power.

Although this stage is comparatively more stable, it continues to affect the supply system, particularly through unbalance and residual harmonics.

2.2. Power quality issues associated with EAF operation

The fluctuating and nonlinear behavior of electric arcs makes EAFs one of the most disturbing industrial loads for electrical networks. Their operation generates a wide spectrum of harmonics, interharmonics, voltage flicker, and phase unbalances [17]. These disturbances can propagate through the supply system, affecting not only the steel plant itself but also other users connected to the same grid. Among the most important power quality indices influenced by EAF operation are:

i) Total harmonic distortion (THD): ratio of the RMS value of all harmonic components to the RMS value of the fundamental component of voltage or current (1), providing a measure of waveform distortion.
ii) Total demand distortion (TDD): ratio of the RMS value of harmonic currents to the maximum demand load current (2), providing a normalized measure of current distortion.
iii) Voltage unbalance factor (VUF): ratio of the negative-sequence component to the positive-sequence component of the fundamental voltage (3), indicating the three-phase asymmetry.

$$THD = \frac{\sqrt{\sum_{i=2}^{N}(V_i)^2}}{V_1} * 100 \quad (1)$$

$$TDD = \frac{\sqrt{\sum_{i=2}^{N}(I_i)^2}}{I_L} * 100 \quad (2)$$

$$VUF = \frac{|V_2^-|}{|V_1^+|} * 100 \quad (3)$$

Where:
i: harmonic order ($i = 2, \dots, N$).
N: highest harmonic order considered.
V_i: rms value of the voltage at harmonic order i (V).
V_1: rms value of the fundamental voltage (V).
I_i: rms value of the current at harmonic order i (A).
I_L: rms value of the maximum demand load current at PCC (A).
V_2^-: negative-sequence voltage component (V).
V_1^+: positive-sequence voltage component (V).

International standards such as IEEE 519-2022 and IEC 61000-3-13 establish maximum admissible limits for these indices, which must be evaluated at the point of common coupling (PCC) [18]. However, in environments with large-scale EAF operation, these limits are frequently exceeded, highlighting the importance of effective mitigation strategies.

3. PROPOSED METHOD

The proposed methodology integrates a hyperbolic model of the EAF with a multi-objective optimization algorithm to determine the optimal tuning of the passive power filter (PPF) parameters. This approach aims to minimize the most critical power quality indices at the PCC of the steel plant, ensuring robust filter performance across different furnace operating conditions. The sequential steps of the methodology are summarized in Figure 2.

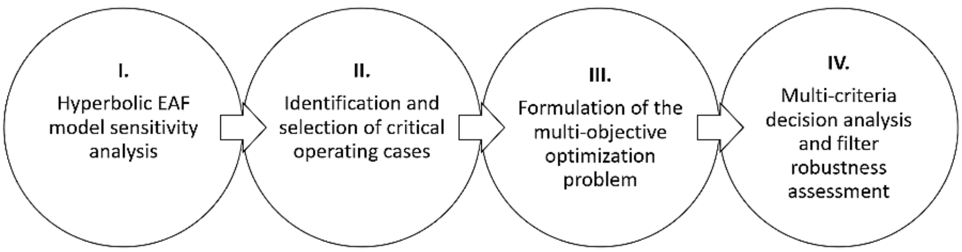

Figure 2. Proposed methodology framework

3.1. Hyperbolic EAF model sensitivity analysis

The analysis of the furnace impact on power quality indices is carried out using a model capable of reproducing the nonlinear and chaotic behavior characteristic of the EAF. For this reason, in this study the hyperbolic model of the EAF [19], [20] was employed, which describes the arc voltage–current relationship through (4)-(6).

$$V_{at}(l_a) = A + B * l_a \tag{4}$$

$$C_v(t) = \frac{1}{2}(C_i - C_e)\, sign(i_a(t))\, \cos(wt) + C_e \tag{5}$$

$$V_a(t) = V_{at}(l_a) + \frac{C_v(t)}{D+|i_a(t)|} \tag{6}$$

Where:
V_{at}: Arc voltage threshold (V).
l_a: Arc length (cm).
C_v: Oscillating arc power (W).
V_a: EAF arc voltage (V).
A: Voltage drop across electrodes (V).
B: Voltage per unit length of arc (V/cm).
C_i: Arc ignition power (W).
C_e: Arc extinction power (W).
i_a: EAF arc current (A).
D: Average arc transition current (A).

In addition, in order to better represent the operational variability of the EAF, the methodology incorporates a sensitivity analysis of the parameters of the hyperbolic model described in (4)-(6). In particular, the characteristic coefficients C_i, C_e, D and the arc length of each phase are modified. This allows the emulation of more realistic operating conditions, such as unequal arc lengths among phases or dynamic changes in arc behavior during the melting process.

Continuing with the sensitivity analysis performed for each of the four main stages of the melting process shown in Figure 1, different operating conditions are simulated in a typical steel plant network. Voltage and current measurements are taken at the PCC. The measurements are processed to calculate the power quality indices under evaluation: THD, TDD, and VUF for each case.

3.2. Identification and selection of critical operating cases

From the database of the sensitivity analysis, the indices of each scenario are normalized with respect to the maximum limit established by the standard, as expressed in (7). Subsequently, the normalized values are weighted and summed to compute the simple composite index (SCI), as defined in (8).

$$\tilde{f}_{k,i} = \frac{f_{k,i}}{L_i} \tag{7}$$

$$SCI_k = \sum_{i=1}^{m} w_i \tilde{f}_{k,i} \quad (k = 1, \dots, N) \tag{8}$$

Where:
$\tilde{f}_{k,i}$: Normalized value of indicator i for case k.
SCI_k: Simple composite index of case k.
N: Total number of simulated cases/scenarios.
$f_{k,i}$: Value of indicator i for case k.
L_i: Regulatory limit of indicator i according to the corresponding standard.
w_i: Weight assigned to index i (with $\sum_{i=1}^{m} w_i = 1$).

The SCI quantifies the proximity of each scenario to the regulatory limits, generating a ranking of criticality that enables the identification of the most unfavorable configurations. In this way, the most critical cases in terms of power quality degradation are selected. These scenarios are then used as the basis for the formulation of the optimization problem.

3.3. Formulation of the multi-objective optimization problem

The optimal tuning of the proposed PPF to improve power quality indices is formulated as a multi-objective optimization problem. The objective is to minimize three functions (9), namely: the minimization of voltage harmonic distortion (10), the reduction of total demand distortion (11), and the decrease of the voltage unbalance factor (12) at the PCC. These objective functions present inherent trade-offs with each other. To ensure robustness, the optimization is performed across different critical operating cases derived from the sensitivity analysis of the EAF model.

$$F(\mathrm{x}) = \begin{bmatrix} F_1(\mathrm{x}) \\ F_2(\mathrm{x}) \\ F_3(\mathrm{x}) \end{bmatrix} ;\ \mathrm{x} = \left[h, Q_C, C_{PPF}, L_{PPF}, Q_f, R_{PPF}\right] \tag{9}$$

$$F_1(\mathrm{x}) = \frac{1}{M}\sum_{k=1}^{M} THD_v^{(k)}(\mathrm{x}) = \frac{1}{M}\sum_{k=1}^{M}\left(\frac{\sqrt{\sum_{i=2}^{N}\left(V_i^{(k)}\right)^2}}{V_1^{(k)}} * 100\right) \tag{10}$$

$$F_2(\mathrm{x}) = \frac{1}{M}\sum_{k=1}^{M} TDD^{(k)}(\mathrm{x}) = \frac{1}{M}\sum_{k=1}^{M}\left(\frac{\sqrt{\sum_{i=2}^{N}\left(I_i^{(k)}\right)^2}}{I_L^{(k)}} * 100\right) \tag{11}$$

$$F_3(\mathrm{x}) = \frac{1}{M}\sum_{k=1}^{M} VUF^{(k)}(\mathrm{x}) = \frac{1}{M}\sum_{k=1}^{M}\left(\frac{\left|V_2^{-(k)}\right|}{\left|V_1^{+(k)}\right|} * 100\right) \tag{12}$$

Where:
k: index of the critical operating case ($k = 1, \dots, M$).
M: number of critical operating cases.
h: tuning harmonic order.
Q_C: reactive power of the filter (Mvar).
C_{PPF}: filter capacitance (F).
L_{PPF}: filter inductance (H).
Q_f: quality factor.
R_{PPF}: filter resistance (Ω).

The implementation incorporates a set of operational constraints, expressed in (13)-(18), which define both the component capacity limits and the admissible ranges of the filter parameters. These constraints ensure that the optimization process yields technically feasible and practically implementable PPF solutions.

$$h^{min} \leq h \leq h^{max} \tag{13}$$

$$Q_c^{min} \leq Q_c \leq Q_c^{max} \tag{14}$$

$$C_F^{min} \leq C_F \leq C_F^{max} \tag{15}$$

$$L_F^{min} \leq L_F \leq L_F^{max} \tag{16}$$

$$Q^{min} \leq Q \leq Q^{max} \tag{17}$$

$$R_F^{min} \leq R_F \leq R_F^{max} \tag{18}$$

The optimization problem is multi-objective, nonlinear, and involves conflicting goals, since not all power quality indices can be minimized simultaneously. To address this, the non-dominated sorting genetic algorithm II (NSGA-II) is employed. NSGA-II was selected over other evolutionary algorithms because of its ability to efficiently handle nonlinear and non-convex search spaces, to maintain a well-distributed Pareto front, and to prevent premature convergence through its crowding distance mechanism [21]. In addition, its proven performance in power system applications reported in the literature makes it particularly suitable for addressing the conflicting objectives of harmonic distortion and voltage unbalance in EAF-based networks. NSGA-II identifies a set of Pareto-optimal solutions by combining three key mechanisms:

a) Selection, crossover and mutation: From a current population P_t (candidate solutions), an offspring population Q_t is generated. Selection favors fitter individuals, crossover combines parents to explore new regions, and mutation introduces variations to preserve diversity and avoid premature convergence.

b) Non-dominated sorting: The combined population $R_t = P_t \cup Q_t$ is classified into successive Pareto fronts (Fr_1, Fr_2, ...) according to dominance. The first front Fr_1 contains all non-dominated solutions, while subsequent fronts include solutions dominated by those in the previous ones, establishing a hierarchy.
c) Crowding distance: To build the next generation P_{t+1}, entire fronts are added sequentially until the population size is met. If the inclusion of a front exceeds the limit, NSGA-II applies crowding distance to select the most diverse individuals, ensuring a well-spread distribution across the objective space.

The overall selection process is summarized in Figure 3, which illustrates how populations are combined, sorted into Pareto fronts, and filtered to construct P_{t+1}.

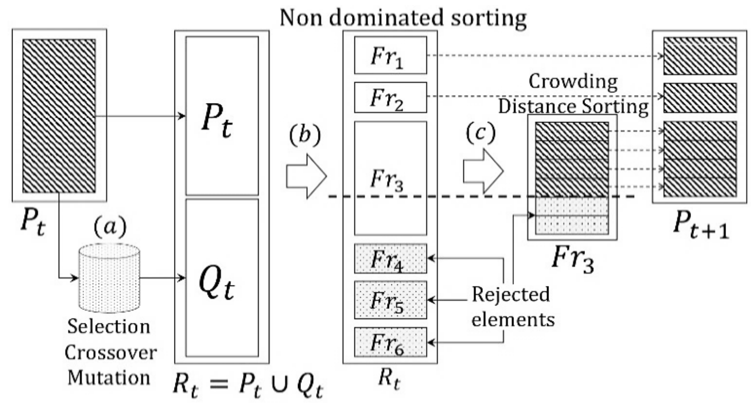

Figure 3. NSGA-II population update process [21]

3.4. Multi-criteria decision analysis and filter robustness assessment

Once the set of optimal solutions (non-dominated front) has been obtained, a multi-criteria decision analysis (MCDA) technique is applied to select the most balanced and robust solution. The MCDA method used in this study is technique for order preference by similarity to ideal solution (TOPSIS), which ranks alternatives according to their relative distance from an ideal solution. This method begins by normalizing and weighting the indices (THD, TDD, VUF) of each candidate solution. Then, the positive ideal and negative ideal solutions are determined using (19), (20), and the Euclidean distances of each alternative to the ideal solutions are calculated using (21), (22).

Afterward, the relative closeness coefficient (CC_i) for each alternative is obtained using (23). This index indicates the proximity to the positive ideal solution and the distance from the negative ideal solution. Thus, the alternative with the highest CC_i is considered the best compromise solution on the Pareto front.

$$A^+ = \{\min(v_{ij})\} \tag{19}$$

$$A^- = \{\max(v_{ij})\} \tag{20}$$

$$D_i^+ = \sqrt{\sum_{j=1}^{n}(v_{ij} - A_j^+)^2} \tag{21}$$

$$D_i^- = \sqrt{\sum_{j=1}^{n}(v_{ij} - A_j^-)^2} \tag{22}$$

$$CC_i = \frac{D_i^-}{D_i^+ + D_i^-} \tag{23}$$

Where:
v_{ij}: normalized and weighted value of criterion j for alternative i.
A^+: positive ideal solution, composed of the minimum values of each criterion.
A^-: negative ideal solution, composed of the maximum values of each criterion.
D_i^+: Euclidean distance of alternative i to the positive ideal solution.
D_i^-: Euclidean distance of alternative i to the negative ideal solution.

Once the optimal configuration of the PPF has been selected, its robustness is evaluated under different operating conditions. The PPF is configured according to the decision variables of the solution chosen by the MCDA method, and its effectiveness is verified in the scenarios defined for the four operating stages of the furnace. New results of power quality indices are then determined and compared with the base case, allowing the assessment of the global effectiveness of the design by evaluating variations in the quality indices obtained in the database. In this way, it is confirmed whether the selected design is robust against the operational variability of the EAF.

4. RESULTS AND DISCUSSION

The application of the proposed methodology follows the procedure summarized in Figure 2, which integrates the sensitivity analysis of the EAF, the formulation and resolution of the optimization problem through NSGA-II, and the application of MCDA for the selection of the most robust filter configuration.

4.1. Case study description

To validate the proposed methodology, a case study was considered based on a steel plant connected to the National Interconnected System of Bolivia, from which the data were obtained. The single-line diagram of the plant under analysis is shown in Figure 4, where the PCC with the external supply network can be observed. The internal network consists of a main transformer T1 rated at 230/11 kV and a transformer T2 rated at 11/0.635 kV supplying the EAF. The electrical parameters of the feeder lines of the circuit are presented in Table 1.

The main load of the plant corresponds to a 19 MW EAF, whose nonlinear characteristic was represented through the hyperbolic model described in section 3.1. To reproduce the variability of the furnace during the melting process, which comprises the stages of boring, melting, plating, and refining, a sensitivity analysis of the model parameters documented in the literature [22]-[24] was carried out. The ranges considered in each stage for this analysis are presented in Table 2.

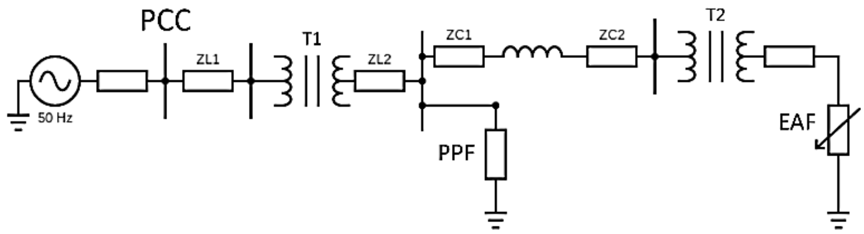

Figure 4. Electrical network of the case study

Table 1. Electrical parameters of the feeder conductors in case-study steel plant network [19]

Feeder	V_N (kV)	I_N (kA)	Length (km)	R' (20 °C) (Ω/km)	X' (Ω/km)
ZL1	230	0.3765	10.7	0.0840	0.4470
ZL2	15	0.5240	0.025	0.0787	0.1511
ZC1	15	0.47	0.03	0.0978	0.1538
ZC2	15	0.47	0.26	0.0978	0.1538

Table 2. Ranges of variation for parameters of the hyperbolic EAF model

Process	l_a (cm)	l_b (cm)	l_c (cm)	C_i	C_e	D
Boring	[25-30-35]	[25-30-35]	[25-30-35]	[150000-250000]	[30000-50000]	[3000-6500]
Melting	[19-23-27]	[19-23-27]	[19-23-27]	[120000-200000]	[24000-40000]	[3500-6000]
Plating	[10-14-18]	[10-14-18]	[10-14-18]	[90000-150000]	[18000-30000]	[4000-5500]
Refining	[3-6-9]	[3-6-9]	[3-6-9]	[60000-100000]	[12000-20000]	[4500-5000]

For each stage, a sensitivity analysis of the hyperbolic model parameters was performed, generating a total of 72 simulated scenarios per stage. Voltages and currents were measured at the PCC in each simulation to calculate the power quality indices under study (THD, TDD, and VUF). The results indicate that the most critical stages are boring and melting, due to their higher distortion and unbalance levels. Figure 5 presents the power quality indices obtained in the base case for the boring stage, highlighting that several of them exceed the limits recommended by international standards.

Finally, in order to select the critical cases that will be used in the optimization stage (see section 3.3), the power quality indices obtained for all simulated scenarios were first normalized with respect to their regulatory limits, as defined in (7). These normalized indices were then weighted and aggregated according to (8) to calculate the SCI for each case. This procedure makes it possible to identify and rank the most critical furnace operating conditions, which are later used as the input set for the optimization process.

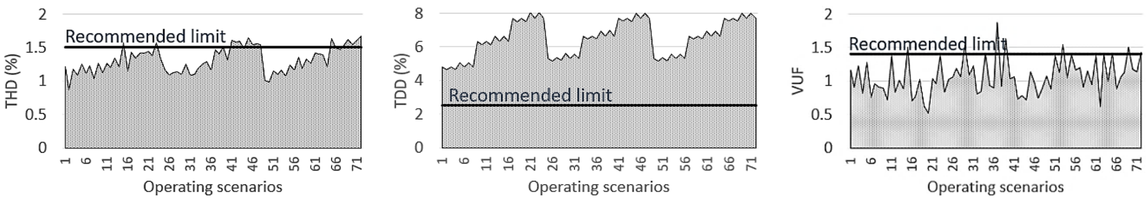

(a) (b) (c)

Figure 5. Power quality indices obtained for the base case in the boring stage: (a) total harmonic distortion, (b) total demand distortion, and (c) voltage unbalance factor

4.2. Multi-objective tuning of the power filter

Based on the database constructed in section 4.1, the multi-objective optimization problem formulated was solved using NSGA-II, implemented in MATLAB 9.13 (R2022b). The optimization problem was formulated with the three objective functions in (10)–(12), while the decision variable limits are summarized in Table 3. The NSGA-II algorithm was configured with a population of 50 individuals, a crossover probability of 0.8, a mutation probability of 0.333, and 100 generations. The optimization produced a Pareto front of non-dominated solutions, illustrating the trade-offs among the objective functions, as shown in Figure 6(a). To select the most balanced alternative, the MCDA approach was applied using (19)–(23) to compute the CC_i for each solution, whose values are presented in Figure 6(b). The alternative with the highest CC_i value (0.3092) was identified as the best compromise solution across the multiple scenarios of the case study. Its corresponding filter parameters are summarized in Table 4, together with those obtained using the conventional tuning method described in [25], [26] for comparison.

Table 3. Decision variable limits

Variable	Lower bound	Upper bound
h	3	11
Q	10	100
C_F (pF)	5.47	100
L_F (H)	3.06	56.13
R_F (Ω)	105.8	5290
Q_c (Mvar)	1	5

Table 4. Filter parameters of the conventional and proposed method

Variable	Conventional method	Proposed method
h	5	4.9184
Q	16	86.2839
C_F (pF)	36.70	54.561
L_F (H)	11.04	7.6766
R_F (Ω)	346.88	137.4720
Q_c (Mvar)	3.05	3.4598

4.3. Validation and comparison of results

Once the optimal filter configuration was identified, its robustness was assessed by extending the simulations to all operating scenarios defined in section 4.1. A comparison of the power quality indices at the PCC, obtained using the proposed and conventional methods during the boring stage, is shown in Figure 7. The results show that the proposed optimization achieves lower harmonic distortion indices (THD, TDD) in all evaluated cases, whereas the conventional design consistently yields higher values. The overall performance of both configurations with respect to the base case (without compensation) is summarized in Table 5, which reports the average values of the power quality indices across the entire furnace process.

Table 5 shows that the proposed optimization-based filter design achieves a 47.6% reduction in THD and a 33.5% reduction in TDD with respect to the base case, while also providing additional decreases of 4.8% in THD and 2.1% in TDD relative to the conventional method. In contrast, although the optimized tuning slightly increases VUF compared with the conventional filter, it still delivers a 63.6% reduction in VUF with respect to the base case and remains well below the maximum permissible value imposed by the standards. Overall, these results indicate that the proposed method yields superior harmonic performance, with the largest relative improvements observed in THD and TDD.

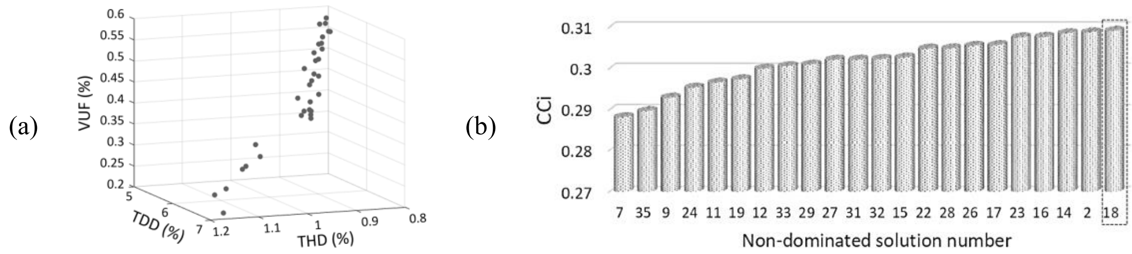

Figure 6. Optimal solution selection via integrated ranking: (a) Pareto front of the case study and (b) CC_i ranking of the non-dominated solutions

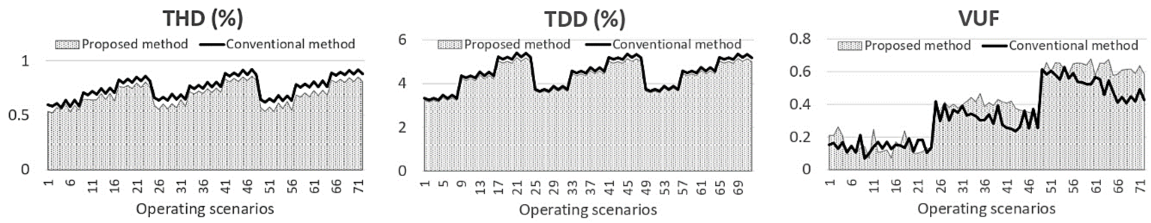

(a) (b) (c)

Figure 7. Comparison of power quality indices between the proposed and conventional methods: (a) total harmonic distortion, (b) total demand distortion, and (c) voltage unbalance factor

Table 5. Comparison of average power quality indices at the PCC

Power quality index	Base case	Conventional method	Proposed method
THD (%)	1.3147	0.7521 (-42.8%)	0.6895 (-47.6%)
TDD (%)	6.4937	4.4547 (-31.4%)	4.3171 (-33.5%)
VUF	1.0637	0.3272 (-69.2 %)	0.3869 (-63.6%)

4.4. Discussion

The results in Table 5 indicate that the optimized filter clearly outperforms both the base case and the conventional PPF. The NSGA-II–based tuning achieves markedly lower THD and TDD over the whole furnace process, confirming its effectiveness in mitigating current harmonics under highly variable EAF operating conditions. In contrast, the average VUF obtained with the optimized design is slightly higher than with the conventional filter, but this increase is modest and VUF remains well below the maximum permissible limit imposed by the standards. These trends suggest that the optimization primarily favors the reduction of TDD and THD over further improvements in VUF, a trade-off that is examined in more detail using the normalized indices in Figure 8.

Figure 8 provides further insight into this trade-off by showing THD, TDD, and VUF normalized with respect to their corresponding regulatory limits. A normalized value greater than 1 indicates that the index exceeds the admissible range, whereas values below 1 denote full compliance with the standards. It can be observed that, in the base case, TDD is the most critical indicator, since it clearly surpasses the limit, while VUF already lies within the acceptable range.

In the proposed methodology, the Pareto-optimal set generated by NSGA-II is post-processed using the MCDA technique TOPSIS. The decision matrix is constructed from the normalized indices and the closeness to the ideal solution is computed, so that solutions with lower normalized THD and TDD (particularly those above the limit) are ranked more favorably. As a result, the selected operating point corresponds to a design that substantially reduces TDD and THD, even if this implies a small increase in VUF. Importantly, VUF remains well below its maximum permissible value, so this trade-off is acceptable from both a technical and regulatory perspective.

Overall, the combined NSGA-II and TOPSIS framework explicitly steers the optimization towards mitigating the most severe non-compliances (mainly TDD), reducing the magnitude of the violation and yielding a more balanced compromise among THD, TDD, and VUF. This regulation-oriented tuning can be regarded as a first step that may be complemented with additional mitigation measures if strict fulfillment of all limits is required.

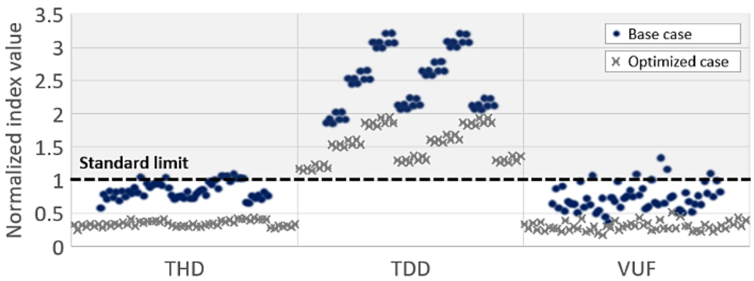

Figure 8. Normalized power quality indices at the PCC relative to the base case

5. CONCLUSION

This paper presented a methodology for optimal tuning of shunt passive filters in EAF-based systems using the NSGA-II multi-objective optimization algorithm, simultaneously minimizing THD, TDD, and VUF. The approach considered the nonlinear and highly variable behavior of the furnace, ensuring filter performance under critical and unbalanced operating scenarios. The results showed that the proposed design clearly outperforms conventional tuning, achieving more effective reductions in power quality indices, especially in scenarios where regulatory limits are exceeded. Moreover, validation across different operating stages confirmed the robustness of the optimized filter under dynamic conditions. Overall, combining evolutionary optimization with decision-making methods provides a resilient strategy to address power quality challenges in steelmaking facilities. As future work, the extension of this methodology to active or hybrid active–passive filters is suggested, as well as its application to other industrial facilities with highly nonlinear loads beyond steelmaking.

FUNDING INFORMATION

This work was supported by the Deutscher Akademischer Austauschdienst (DAAD) under a postgraduate scholarship.

AUTHOR CONTRIBUTIONS STATEMENT

This journal uses the Contributor Roles Taxonomy (CRediT) to recognize individual author contributions, reduce authorship disputes, and facilitate collaboration.

Name of Author	C	M	So	Va	Fo	I	R	D	O	E	Vi	Su	P	Fu
Alvaro Yassif Marca Yucra	✓	✓	✓	✓	✓	✓		✓	✓		✓		✓	✓
Gastón Orlando Suvire	✓	✓		✓	✓	✓	✓			✓		✓		
John Armando Morales	✓	✓		✓	✓	✓	✓			✓		✓		

C : **C**onceptualization
M : **M**ethodology
So : **So**ftware
Va : **Va**lidation
Fo : **Fo**rmal analysis
I : **I**nvestigation
R : **R**esources
D : **D**ata Curation
O : Writing - **O**riginal Draft
E : Writing - Review & **E**diting
Vi : **Vi**sualization
Su : **Su**pervision
P : **P**roject administration
Fu : **Fu**nding acquisition

CONFLICT OF INTEREST STATEMENT

The authors declare that they have no conflict of interest.

DATA AVAILABILITY

The data supporting the findings of this study are available within the article.

REFERENCES

[1] I. R. S. Filho *et al.*, "Green steel at its crossroads: hybrid hydrogen-based reduction of iron ores," *Journal of Cleaner Production*, vol. 340, p. 130805, Mar. 2022, doi: 10.1016/j.jclepro.2022.130805.

[2] J. Suer, F. Ahrenhold, and M. Traverso, "Carbon footprint and energy transformation analysis of steel produced via a direct reduction plant with an integrated electric melting unit," *Journal of Sustainable Metallurgy*, vol. 8, no. 4, pp. 1532–1545, Dec. 2022, doi: 10.1007/s40831-022-00585-x.

[3] J. Suer, M. Traverso, and N. Jäger, "Review of life cycle assessments for steel and environmental analysis of future steel production scenarios," *Sustainability*, vol. 14, no. 21, p. 14131, Oct. 2022, doi: 10.3390/su142114131.

[4] Z. Łukasik and Z. Olczykowski, "Estimating the impact of arc furnaces on the quality of power in supply systems," *Energies*, vol. 13, no. 6, p. 1462, Mar. 2020, doi: 10.3390/en13061462.

[5] X. Zhu, H. Chen, P. Hu, and R. Chen, "Reactive compensation for ac electric arc furnace considering power quality constraints," in *2016 17th International Conference on Harmonics and Quality of Power (ICHQP)*, IEEE, Oct. 2016, pp. 919–924, doi: 10.1109/ICHQP.2016.7783453.

[6] Z. Olczykowski, "Arc voltage distortion as a source of higher harmonics generated by electric arc furnaces," *Energies*, vol. 15, no. 10, p. 3628, May 2022, doi: 10.3390/en15103628.

[7] W. Yugcha, D. Pichoasamin, and P. Astudillo, "Comparación y optimización del uso de filtro pasivo y activo de potencia para mitigar armónicos en redes de distribución con cargas no lineal," *Revista Técnica "energía,"* vol. 21, no. 1, pp. 1–11, 2024, doi: 10.37116/revistaenergia.v21.n1.2024.632.

[8] S. H. E. A. Aleem, A. F. Zobaa, and M. M. A. Aziz, "Optimal C-type passive filter based on minimization of the voltage harmonic distortion for nonlinear loads," *IEEE Transactions on Industrial Electronics*, vol. 59, no. 1, pp. 281–289, Jan. 2012, doi: 10.1109/TIE.2011.2141099.

[9] L. I. Kovernikova and N. C. Thanh, "An optimization approach to calculation of passive filter parameters based on particle swarm optimization," *RE&PQJ*, vol. 10, no. 4, Jan. 2024, doi: 10.24084/repqj10.396.

[10] J. Ji, H. Liu, G. Zeng, and J. Zhang, "The multi-objective optimization design of passive power filter based on PSO," in *2012 Asia-Pacific Power and Energy Engineering Conference*, IEEE, Mar. 2012, pp. 1–4, doi: 10.1109/APPEEC.2012.6307477.

[11] V. R. Pandi, H. H. Zeineldin, and W. Xiao, "Passive harmonic filter planning to overcome power quality issues in radial distribution systems," in *2012 IEEE Power and Energy Society General Meeting*, IEEE, Jul. 2012, pp. 1–6, doi: 10.1109/PESGM.2012.6345247.

[12] A. M. Sharaf and A. A. A. El-Gammal, "A discrete particle swarm optimization technique (DPSO) for power filter design," in *2009 4th International Design and Test Workshop (IDT)*, IEEE, Nov. 2009, pp. 1–6, doi: 10.1109/IDT.2009.5404376.

[13] Y.-Y. Hong and C.-S. Chiu, "Passive filter planning using simultaneous perturbation stochastic approximation," *IEEE Transactions on Power Delivery*, vol. 25, no. 2, pp. 939–946, Apr. 2010, doi: 10.1109/TPWRD.2009.2035701.

[14] S. A. L. Serrano, J. L. P. Durán, J. V. Oyaga, and C. A. T. Pinzón, "Evaluación de filtros pasivos para la gestión de armónicos en redes industriales de distribución eléctrica," *TecnoLógicas*, vol. 26, no. 58, p. e2839, Dec. 2023, doi: 10.22430/22565337.2839.

[15] J. Madias, "Electric arc furnace," in *Ironmaking and Steelmaking Processes*, Cham: Springer International Publishing, 2016, pp. 267–281, doi: 10.1007/978-3-319-39529-6_16.

[16] M. Karbowniczek, *Electric arc furnace steelmaking*. CRC Press, 2021. [Online]. Available: https://www.perlego.com/book/2806536/electric-arc-furnace-steelmaking-pdf.

[17] K. U. Vinayaka and P. S. Puttaswamy, "Review on characteristic modeling of electric arc furnace and its effects," in *2017 International Conference on Intelligent Computing, Instrumentation and Control Technologies (ICICICT)*, IEEE, Jul. 2017, pp. 1222–1229, doi: 10.1109/ICICICT1.2017.8342744.

[18] P. M. Balasubramaniam and S. U. Prabha, "Power quality issues, solutions and standards: a technology review," *Journal of Applied Science and Engineering*, vol. 18, no. 4, pp. 371–380, 2015, doi: 10.6180/jase.2015.18.4.08.

[19] J. C. G. Arispe and A. Y. M. Yucra, "Análisis de armónicos en sistemas eléctricos de potencia y normas regulatorias: impacto del horno de arco eléctrico de acerías," *Ingeniare. Revista chilena de ingeniería*, vol. 32, May 2024, doi: 10.4067/S0718-33052024000100201.

[20] C. G. Castaño, A. A. Gómez, and J. J. M. Durango, "Modelos de horno de arco eléctrico para estudios del efecto flicker," *Revista Tecnura*, vol. 20, no. 48, pp. 15–27, 2016, doi: 10.14483/udistrital.jour.tecnura.2016.2.a01.

[21] J. Liu and X. Chen, "An improved NSGA-II algorithm based on crowding distance elimination strategy," *International Journal of Computational Intelligence Systems*, vol. 12, no. 2, pp. 513–518, 2019, doi: 10.2991/ijcis.d.190328.001.

[22] R. H. G. Tan and V. K. Ramachandaramurthy, "A comprehensive modeling and simulation of power quality disturbances using MATLAB/Simulink," in *Power Quality Issues in Distributed Generation*, 2015, doi: 10.5772/61209.

[23] D. C. Bhonsle and R. B. Kelkar, "New time domain electric arc furnace model for power quality study," in *2014 IEEE 6th India International Conference on Power Electronics (IICPE)*, IEEE, Dec. 2014, pp. 1–6, doi: 10.1109/IICPE.2014.7115761.

[24] M. Banejad, R.-A. Hooshmand, and M. Torabian E, "Exponential-hyperbolic model for actual operating conditions of three phase arc furnaces," *American Journal of Applied Sciences*, vol. 6, no. 8, pp. 1539–1547, Aug. 2009, doi: 10.3844/ajassp.2009.1539.1547.

[25] W. Ko and M. Tuomainen, "Design and application of a single-tuned passive harmonic filter to suppress harmonic distortion and resonance for railway traction power systems—a case study," *IET Electrical Systems in Transportation*, vol. 12, no. 2, pp. 153–164, Jun. 2022, doi: 10.1049/els2.12041.

[26] M. Ahmed, N. Al Masood, and T. Aziz, "Optimal selection of single tuned passive filters to enhance post-fault voltage recovery and power quality in a renewable integrated microgrid," *IET Renewable Power Generation*, vol. 17, no. 7, pp. 1747–1767, 2023, doi: 10.1049/rpg2.12710.

BIOGRAPHIES OF AUTHORS

Alvaro Yassif Marca Yucra is a Ph.D. candidate and DAAD scholarship holder at the Institute of Electrical Energy (IEE), Universidad Nacional de San Juan (UNSJ), Argentina. He received the B.Sc. degree in electrical engineering from Universidad Mayor de San Simón (UMSS), Cochabamba, Bolivia, in 2020, and the M.Sc. degree in higher education for innovation in diversity from the same university in 2022. His research interests include harmonic analysis, power quality, energy efficiency, and power converters. He can be contacted at email: alvaromarca25@gmail.com.

Gastón Orlando Suvire graduated as an electric engineer from the National University of San Juan (UNSJ), Argentina, in 2002. He received his Ph.D. from the same University in 2009, carrying out part in the COPPE institute, in the Federal University of Rio de Janeiro in Brazil. From 2009 to 2012, he worked as a postdoctoral research fellow from Argentinean National Council for Science and Technology Research (CONICET) at the Institute of Electrical Energy, UNSJ. In 2017, he worked as a postdoctoral research fellow from the "Visiting Fulbright Scholar Program" between CONICET and the Fulbright Commission, in the Pacific Northwest National Laboratory (PNNL) - U.S. Department of Energy. He is currently a professor of electrical engineering at the UNSJ and a researcher with CONICET. His research interests include simulation methods, power systems dynamics and control, and power electronics modeling and design. He can be contacted at email: gsuvire@iee-unsjconicet.org.

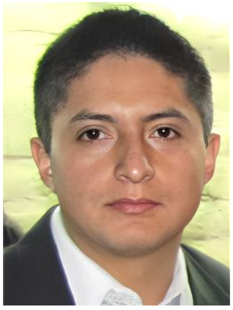

John Armando Morales graduated as an electric engineer from Universidad Politécnica Salesiana, Cuenca, Ecuador, in 2008. From 2010 to 2014, he pursued doctoral studies at the Institute of Electrical Energy (IEE), Universidad Nacional de San Juan (UNSJ), Argentina, where he obtained the Ph.D. degree in electrical engineering. His research interests include power system protection, signal processing applied to electric power systems, electromagnetic transient simulation, and electromagnetism. He has authored and coauthored more than 40 scientific publications in indexed journals and international conferences. He has also participated in different research projects and contributed to the training of undergraduate and doctoral students. He can be contacted at email: jmorales@iee-unsjconicet.org.